TAp73 suppresses tumor angiogenesis through repression of proangiogenic cytokines and HIF-1α activity

Marina Stantic[a], Habib A. M. Sakil[a], Hanna Zirath[a], Trixy Fang[a], Gema Sanz[a], Alejandro Fernandez-Woodbridge[a], Ana Marin[a], Evelyn Susanto[a], Tak W. Mak[b,1], Marie Arsenian Henriksson[a], and Margareta T. Wilhelm[a,1]

[a]Department of Microbiology, Tumor and Cell Biology, Karolinska Institutet, 171 77 Stockholm, Sweden; and [b]The Campbell Family Cancer Research Institute, Ontario Cancer Institute, University Health Network, Toronto, Ontario M5G 2C1, Canada

Contributed by Tak W. Mak, November 19, 2014 (sent for review August 8, 2014)

The p53-family member TAp73 is known to function as a tumor suppressor and regulates genomic integrity, cellular proliferation, and apoptosis; however, its role in tumor angiogenesis is poorly understood. Here we demonstrate that TAp73 regulates tumor angiogenesis through repression of proangiogenic and proinflammatory cytokines. Importantly, loss of TAp73 results in highly vascularized tumors, as well as an increase in vessel permeability resulting from disruption of vascular endothelial-cadherin junctions between endothelial cells. In contrast, loss of the oncogenic p73 isoform ΔNp73 leads to reduced blood vessel formation in tumors. Furthermore, we show that up-regulated ΔNp73 levels are associated with increased angiogenesis in human breast cancer and that inhibition of TAp73 results in an accumulation of HIF-1α and up-regulation of HIF-1α target genes. Taken together, our data demonstrate that loss of TAp73 or ΔNp73 up-regulation activates the angiogenic switch that stimulates tumor growth and progression.

p73 | angiogenesis | HIF-1 alpha | tumor microenvironment | vascular permeability

The *TP73* gene belongs to the p53 tumor suppressor family and encodes two different classes of proteins: full-length isoforms (TAp73) that act as transcription factors and N-terminal truncated isoforms transcribed from an internal promoter (ΔNp73) or by aberrant splicing of TAp73 mRNA (TAp73Δex2, TAp73Δex2/3, and ΔN′, collectively called ΔTAp73 isoforms). The ΔN and ΔTAp73 isoforms block the transactivation activity of the full-length proteins in a dominant-negative fashion, thus acting like oncogenes. Furthermore, alternative splicing of C-terminal exons adds additional isoforms (TAp73α–η and ΔNp73α–η) (1).

Among the p73 isoforms, TAp73 is known to function as a tumor suppressor and shares many hallmark features with the archetypical tumor suppressor p53. TAp73 induces cell cycle arrest, apoptosis, and differentiation, whereas antiapoptotic ΔNp73 competes with TAp73 and p53 for DNA binding to same-target promoters or oligomerizes with and sequesters TAp73 (2). Furthermore, TAp73 has been found to control genomic stability through regulation of the spindle assembly checkpoint, and mice deficient for TAp73 spontaneously develop tumors as a result of mitotic abnormalities (3, 4). Recent studies have shown that TAp73 also acts as an inhibitor of tumor cell migration and invasion (5, 6). However, in contrast to *TP53*, the *TP73* gene is rarely mutated. Instead TAp73 isoforms are found silenced through promoter methylation in hematological malignancies, including acute lymphoblastic leukemia, Burkitt's lymphoma, and natural killer cell lymphomas (7–9). In contrast, ΔNp73 impairs the DNA damage response; supports cellular transformation, tumor invasion, and metastasis (10–12); and is found up-regulated in several types of solid cancer, including medulloblastoma, breast, ovarian, lung, and colon cancer (13–16).

Angiogenesis, the formation of new blood vessels, plays a critical role for the maintenance, growth, and spread of tumor cells and is considered one of the hallmarks of cancer. The role of p73 during tumor angiogenesis is poorly understood, but aberrant expression of the *p73* locus has been correlated with enhanced tumor vascularization in both colon and breast cancer (17, 18). Here we report that TAp73 and ΔNp73 have opposing roles during tumor angiogenesis. Loss of TAp73 promotes blood vessel formation through up-regulation of proangiogenic and proinflammatory cytokines, whereas ΔNp73-deficient tumors show a reduction in angiogenesis. Furthermore, we show that up-regulation of ΔNp73 correlates with increased angiogenesis in human breast cancer and that inhibition of TAp73 results in an accumulation of Hif-1α protein and activation of proangiogenic Hif-1α target genes.

Results

TAp73 Loss Enhances Anchorage-Independent Growth of Transformed Cells in Vitro and Tumor Growth and Angiogenesis in Vivo. We have previously shown that loss of ΔNp73 impairs tumor development in vivo (11). To investigate the effect of TAp73 deficiency on tumorigenesis, we transformed TAp73$^{+/+}$ and TAp73$^{-/-}$ primary mouse embryonic fibroblasts with E1A and H-Ras^{V12} (MEF$^{E1A/Ras}$) (Fig. S1*A*). No difference was found in proliferation rate in vitro (Fig. S1 *B* and *C*); however, we observed an enhanced capacity of TAp73$^{-/-}$-transformed cells for anchorage-independent growth (Fig. S1 *D* and *E*). This supports previous data showing that TAp73 knockdown (KD) by siRNA confers anchorage-independent growth to BJ-TE human fibroblasts (19). To study how TAp73 controls the establishment of tumors in vivo, transformed MEFs were injected

Significance

Angiogenesis, the development of blood vessels within a solid tumor, is not only essential for primary tumor growth but also vital for tumor invasion and metastasis. The *TP73* gene, a p53-family gene, encodes for both a tumor suppressor, TAp73, and an oncogene, ΔNp73. Here we report that TAp73 and ΔNp73 have opposing roles in tumor angiogenesis. Loss of TAp73 or upregulation of ΔNp73 leads to highly vascularized tumors and is found to correlate with increased angiogenesis in patients with breast cancer. Furthermore, we show that TAp73 suppress proangiogenic cytokines and HIF-1α protein accumulation and that this repression is unleashed on TAp73 loss or ΔNp73 up-regulation, thus further fuelling tumor development.

Author contributions: T.W.M., M.A.H., and M.T.W. designed research; M.S., H.A.M.S., H.Z., T.F., G.S., A.F.-W., A.M., E.S., and M.T.W. performed research; T.W.M. contributed new reagents/analytic tools; M.S., H.A.M.S., H.Z., T.F., G.S., A.F.-W., A.M., E.S., and M.T.W. analyzed data; and M.S., H.A.M.S., and M.T.W. wrote the paper.

The authors declare no conflict of interest.

Freely available online through the PNAS open access option.

[1]To whom correspondence may be addressed. Email: margareta.wilhelm@ki.se or tmak@uhnresearch.ca.

This article contains supporting information online at www.pnas.org/lookup/suppl/doi:10.1073/pnas.1421697112/-/DCSupplemental.

www.pnas.org/cgi/doi/10.1073/pnas.1421697112

s.c. into athymic nude mice. TAp73-deficient MEFs$^{E1A/Ras}$ formed larger tumors with shorter latency compared with WT (Fig. 1 *A* and *B*), indicating that loss of TAp73 confers tumor cells a growth advantage in vivo. Strikingly, we observed that the TAp73$^{-/-}$ tumors had a more vascularized appearance compared with WT, and immunofluorescence staining using blood vessel marker endomucin revealed extensive angiogenesis (Fig. 1 *C* and *E*). In light of these results, we investigated the angiogenic phenotype in tumors derived previously from ΔNp73$^{-/-}$ MEF$^{E1A/Ras}$ cells (11) and observed a reduction in blood vessel formation, indicating that ΔNp73 positively regulates angiogenesis (Fig. 1 *D* and *F*). To validate our findings in a spontaneous tumor model, the TAp73$^{-/-}$ and ΔNp73$^{-/-}$ mice were crossed to the EμMyc B-cell lymphoma model (20). In agreement with the E1A/Ras model, we found more blood vessel formation in lymphomas from TAp73$^{-/-}$/EμMyc and less in ΔNp73$^{-/-}$/EμMyc compared with p73$^{+/+}$/EμMyc mice (Fig. 1 *G*, *H*, *J*, and *K*). Taken together, this suggests that p73 isoforms have opposing roles in regulating tumor angiogenesis.

p73 Isoforms Have Opposite Effect on Endothelial Cell Sprouting in Vivo. To determine whether the effect of p73 isoforms on tumor angiogenesis is a result of factors produced by the tumor cells and not tumor size, we used a short-term xenograft model using *Tg(fli:EGFP)* transgenic zebrafish (21). In this model, green fluorescent protein (EGFP) is expressed throughout the vasculature, allowing for visualization of tumor cell interactions with endogenous endothelial cells in vivo. Zebrafish embryos were injected with fluorescently labeled WT, TAp73$^{-/-}$, or ΔNp73$^{-/-}$ MEFs$^{E1A/Ras}$ and scored for endothelial cell sprouting 20 h after injection (Fig. 1*I*). Consistent with our previous results, we observed an almost twofold increase in angiogenic response toward TAp73$^{-/-}$ cells compared with WT cells (Fig. 1*L*). In contrast, ΔNp73-deficient cells elicited a twofold decrease in angiogenic sprouting (Fig. 1*L*), demonstrating that p73 isoforms have opposing function in regulating tumor angiogenesis by directly affecting endothelial cell sprouting.

TAp73-Deficient Tumor Cells Increase Blood Vessel Permeability Through Disruption of Endothelial Vascular Endothelial-Cadherin Junctions. Normally, a mature blood vessel endothelium functions as a barrier that limits vascular leakage. However, tumor cells stimulate endothelial cells to start to proliferate, migrate, and become more permeable (22). Considering the enhanced effect on endothelial cell sprouting, we next investigated the effect of

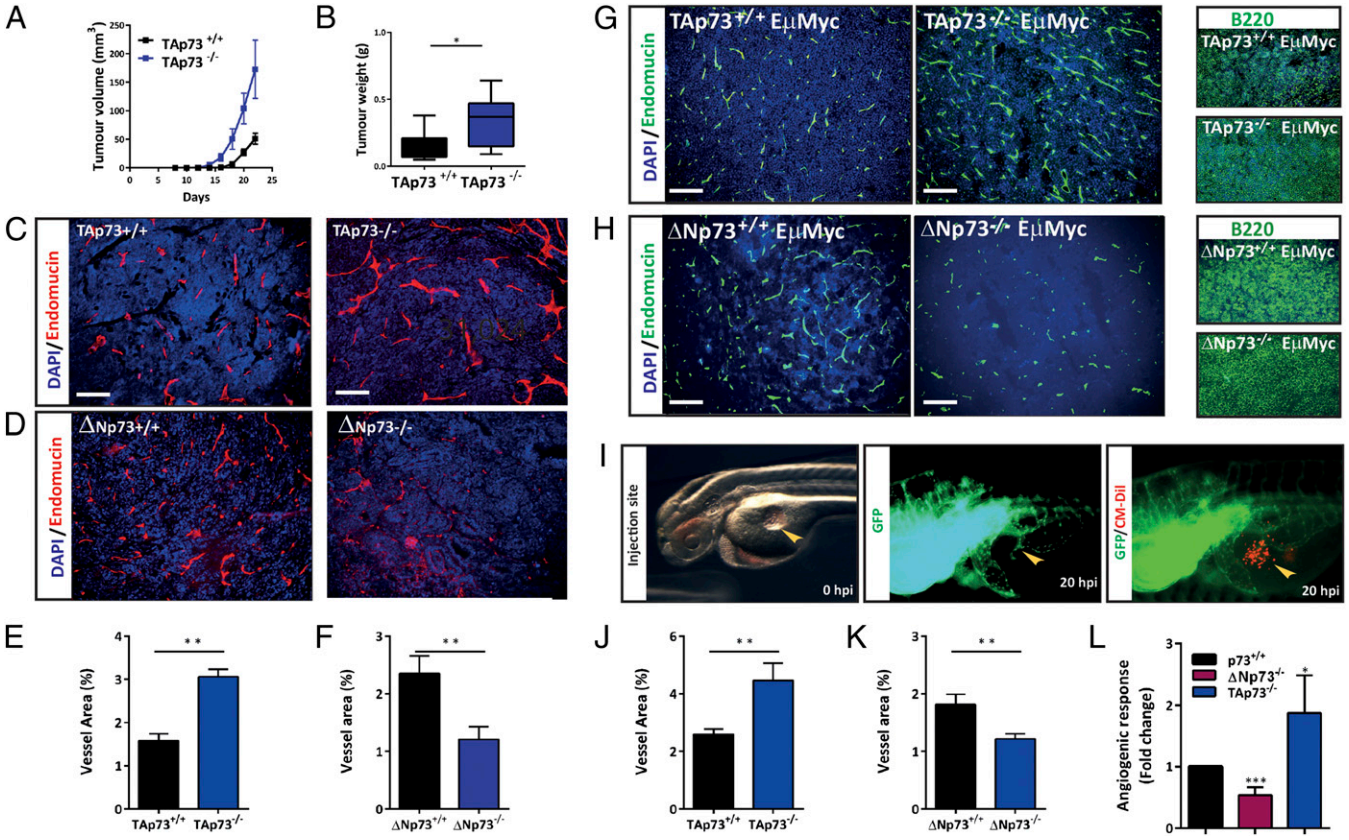

Fig. 1. TAp73-deficient cells form larger and more vascularized tumors compared with WT. (*A*) E1A/Ras^{V12}-transformed WT or TAp73$^{-/-}$ MEFs were injected s.c. into nude mice (n = 9/group), tumor growth was measured at a 2-d interval up to 22 d postinjection. Results are shown as the mean ± SEM, $P < 0.0001$. (*B*) Increased tumor weight in absence of TAp73 (TAp73$^{-/-}$, 0.33 ± 0.07 g vs. WT, 0.14 ± 0.045 g; $*P < 0.05$) Results are shown as the mean ± SD. (*C*–*F*) Representative images and quantification of tumor vasculature in WT, TAp73$^{-/-}$, and ΔNp73$^{-/-}$ tumors using anti-endomucin staining (red) on paraffin sections. In total, n = 14 TAp73$^{-/-}$, n = 12 TAp73$^{+/+}$, n = 4 ΔNp73$^{-/-}$, and n = 4 ΔNp73$^{+/+}$ tumors were analyzed and five fields/tumor were used for quantification. (*G*, *H*, *J*, and *K*) Images and quantification of vasculature in spontaneous B-cell lymphoma model in TAp73$^{-/-}$ (n = 3), ΔNp73$^{-/-}$ (n = 3), and WT (n = 3) tumors, using anti-endomucin staining (green) on paraffin sections. Five to 10 fields per tumor were used for quantification ($**P < 0.01$). (*Right*) B220 staining indicating all tumors analyzed are of B-cell origin. (*I*) Tumor cell xenografts into zebrafish embryos. (*Left*) 48 h postfertilization (hpf) Tg(fli:EGFP) embryos injected with CM-DiI–labeled MEFs$^{E1A/Ras}$ into the perivitelline space. (*Middle*) Injected embryo stage 72 hpf (20 h after injection) with a positive angiogenic response (arrowhead). (*Right*) Overlay with grafted cells (red). (*L*) Quantification of angiogenic response in zebrafish comparing three WT cell lines with three ΔNp73$^{-/-}$ or three TAp73$^{-/-}$ cell lines (all generated from paired litter mates). Results are presented as mean fold change ± SD compared with WT. Cells deficient for ΔNp73 show a reduced angiogenic response compared with WT [0.54 ± 0.06 vs. 1 (WT); $***P < 0.0005$]; in contrast, TAp73$^{-/-}$ cells show an enhanced response [1.88 ± 0.35 vs. 1 (WT); $*P < 0.05$].

TAp73 loss on blood vessel permeability. Nude mice bearing TAp73$^{+/+}$ or TAp73$^{-/-}$ MEF$^{E1A/Ras}$ tumors of similar size were injected with FITC-labeled high-molecular dextran. We observed more FITC-dextran leakage into the extravascular space in TAp73$^{-/-}$ tumors compared with in WT tumors, demonstrating that blood vessels in TAp73$^{-/-}$-derived tumors have increased vascular permeability (Fig. 2 *A* and *B*). To determine whether this increase is caused by factors directly produced by TAp73$^{-/-}$ tumor cells, we cultured TAp73$^{-/-}$ and TAp73$^{+/+}$ MEF$^{E1A/Ras}$ cells in hypoxia to mimic the tumor microenvironment and collected conditioned media (CM). The CM was added to confluent human dermal microvascular endothelial cells (HuDMEC) to analyze the effect on endothelial cell–cell contact (Fig. 2*C*). Using scanning electron microscopy (SEM), we found that HuDMECs exposed to TAp73$^{+/+}$ MEF$^{E1A/Ras}$ CM still retain interendothelial bonds. In contrast, cells treated with TAp73$^{-/-}$ MEF$^{E1A/Ras}$ CM show a dramatic loss in interconnecting network, resulting in more gaps between the endothelial cells. This indicates that in hypoxic conditions, TAp73$^{-/-}$ tumor cells are producing factors that decrease the cell–cell contact between endothelial cells, thus increasing blood vessel permeability (Fig. 2*D*). Endothelial cell–cell junctions are regulated by a variety of extracellular stimuli, which often lead to reorganization of interendothelial contact proteins, such as vascular endothelial (VE)-cadherin (23). Using immunofluorescence, we observed a robust reduction in VE-cadherin signal on the cell surface as well as disruption of cell contact between HuDMECs treated with CM from TAp73$^{-/-}$ MEF$^{E1A/Ras}$ cells exposed to hypoxia (Fig. 2 *E* and *F*), suggesting that TAp73-deficient tumor cells produce and secrete factors that disrupt endothelial cell–cell contact through reducing the cell surface localization of VE-cadherin.

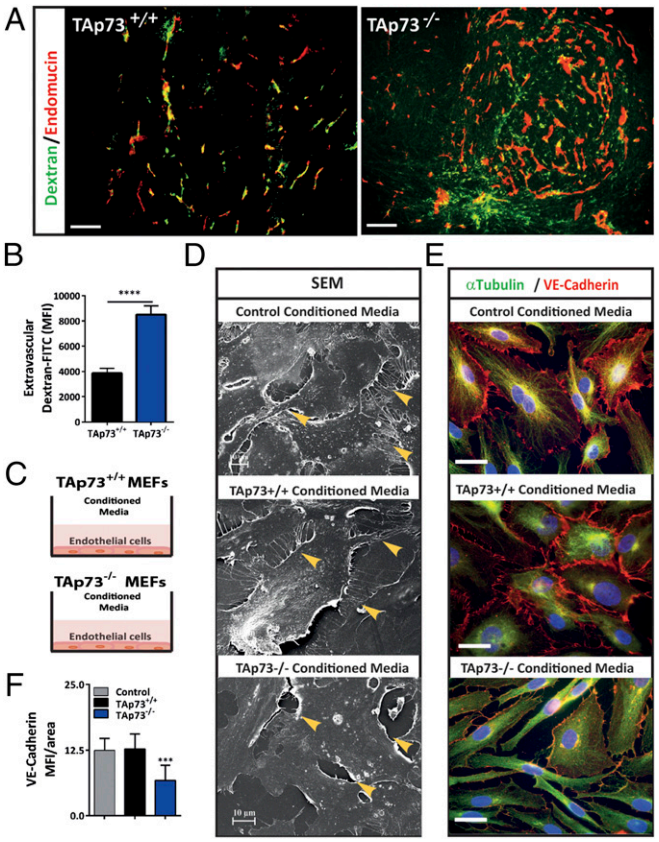

Fig. 2. Loss of TAp73 increases tumor blood vessel permeability through reduced endothelial cell–cell contact. (*A* and *B*) TAp73$^{+/+}$ and TAp73$^{-/-}$ tumors perfused with FITC-labeled dextran and stained for endothelial cells (endomucin). Green, FITC-labeled dextran leakage into the extravascular tumor space; red, endomucin staining of blood vessels. Mean fluorescent intensity (MFI) was determined for total dextran-FITC (green) signal with pixel counting; intravascular dextran-FITC (yellow) was subtracted from the final value (n = 5/group, five fields/tumor was used for quantification; ****P < 0.0001). (Scale bar, 100 μm.) (*C*) Schematic representation of in vitro cell permeability assay. (*D*) SEM of confluent monolayer HuDMECs treated with CM from hypoxic TAp73$^{+/+}$ or TAp73$^{-/-}$MEFs$^{E1A/Ras}$ (*Middle* and *Bottom*) or control HuDMEC media (*Top*). (*Top* and *Middle*) Arrow indicating well-defined junctions and cell–cell contact. (*Bottom*) Breaks in cell–cell contact and gaps between HuDMECs treated with CM from hypoxic TAp73$^{-/-}$MEFs$^{E1A/Ras}$. (Scale bar, 10 μm.) (*E* and *F*) VE–cadherin (red) immunofluorescence staining and quantification. (Scale bar, 50 μm.) (*Top* and *Middle*) HuDMECs treated with control media or CM from hypoxic TAp73$^{+/+}$ MEFs$^{E1A/Ras}$ present distinct interendothelial VE-cadherin bonds and close cell–cell contact. (*Bottom*) Interendothelial VE-cadherin bonds are lost, resulting in weakened cell–cell contact in HuDMECs treated with CM from hypoxic TAp73$^{-/-}$ MEFs$^{E1A/Ras}$.

Enhanced Angiogenic Response in TAp73-Deficient Tumors Is a Result of Increased Expression of Both Proangiogenic and Proinflammatory Genes. To identify target genes involved in angiogenesis and vascular homeostasis regulated by TAp73, we profiled TAp73$^{-/-}$ and TAp73$^{+/+}$ tumors, using a commercial angiogenesis RT^2 profiler PCR array. Among the 84 genes analyzed, 13 showed a significantly up- or down-regulation (≥twofold difference; P value ≤ 0.05) in TAp73-deficient tumors (Fig. 3 *A* and *B*; full list, Table S1), and nine of the potential target genes were validated to be deregulated in TAp73-deficient tumors (Fig. 3*C*). Their expression was mostly reversed in ΔNp73$^{-/-}$ tumors (Fig. 3*D*). To investigate whether the enhanced expression of proangiogenic genes originated from the tumor cells themselves or from the tumor stroma, we analyzed the expression of our genes of interest in TAp73$^{-/-}$, ΔNp73$^{-/-}$, and WT MEFs$^{E1A/Ras}$ grown both in normoxic and hypoxic conditions in vitro (Fig. 3 *E* and *F*). Among genes up-regulated in TAp73$^{-/-}$ cells, we found proinflammatory chemokines known to promote both angiogenesis and leukocyte migration (*Ccl2*, *Cxcl1*, *Cxcl2*), suggesting that TAp73 loss creates a proinflammatory milieu within the tumor. In addition, the proangiogenic genes *Vegfc*, *Ereg*, and *Tnfaip2* were shown to be up-regulated in TAp73$^{-/-}$ cells. VEGF-C and epiregulin (*Ereg*) are both known to induce angiogenesis by promoting endothelial cell proliferation (24, 25). Furthermore, VEGF-C also induces vessel permeability (26). Interestingly, their expression was even further potentiated in hypoxia (Fig. 3*E*).

The proangiogenic expression was reversed on ectopic expression of TAp73β in TAp73$^{-/-}$ MEF$^{E1A/Ras}$ cells, as well as in human MCF7 breast adenocarcinoma cells, showing that TAp73 indeed is suppressing proangiogenic genes (Fig. S2 *A–D*). Intriguingly, ΔNp73$^{-/-}$ MEF$^{E1A/Ras}$ cells only have reduced expression of *Ccl2*, *Cxcl1*, and *Cxcl2* in hypoxia (Fig. 3*F*), suggesting that ΔNp73 enhances expression of these chemokines specifically in low-oxygen conditions. Reintroduction of ΔNp73, and especially ΔNp73α, into ΔNp73$^{-/-}$ cells restored the expression of most cytokines (Fig. S2 *E* and *F*). Next, we examined the effect of TAp73 KD in human H1299 nonsmall cell lung carcinoma cells with stable shRNA KD of TAp73, as well as MDA-MB-231 breast adenocarcinoma cells treated with siRNA against TAp73. Again, we observed an up-regulation of several proangiogenic factors, especially CCL2, CXCL1, CXCL2, and VEGF-C, on TAp73 KD (Fig. 3 *G* and *F*). We did not observe any significant effect on ΔNp73 levels on TAp73 KD or loss in the cell lines we used, showing the isoform-specificity of the KD (Fig. S3). Taken together, our findings show that TAp73 suppress the production of proangiogenic factors and that loss of TAp73 or ΔNp73 overexpression releases this repression, thus increasing tumor angiogenesis.

Importantly, the only gene significantly down-regulated in TAp73$^{-/-}$ and, conversely, up-regulated in ΔNp73$^{-/-}$ tumors and cells compared with WT was brain-specific angiogenesis inhibitor-1

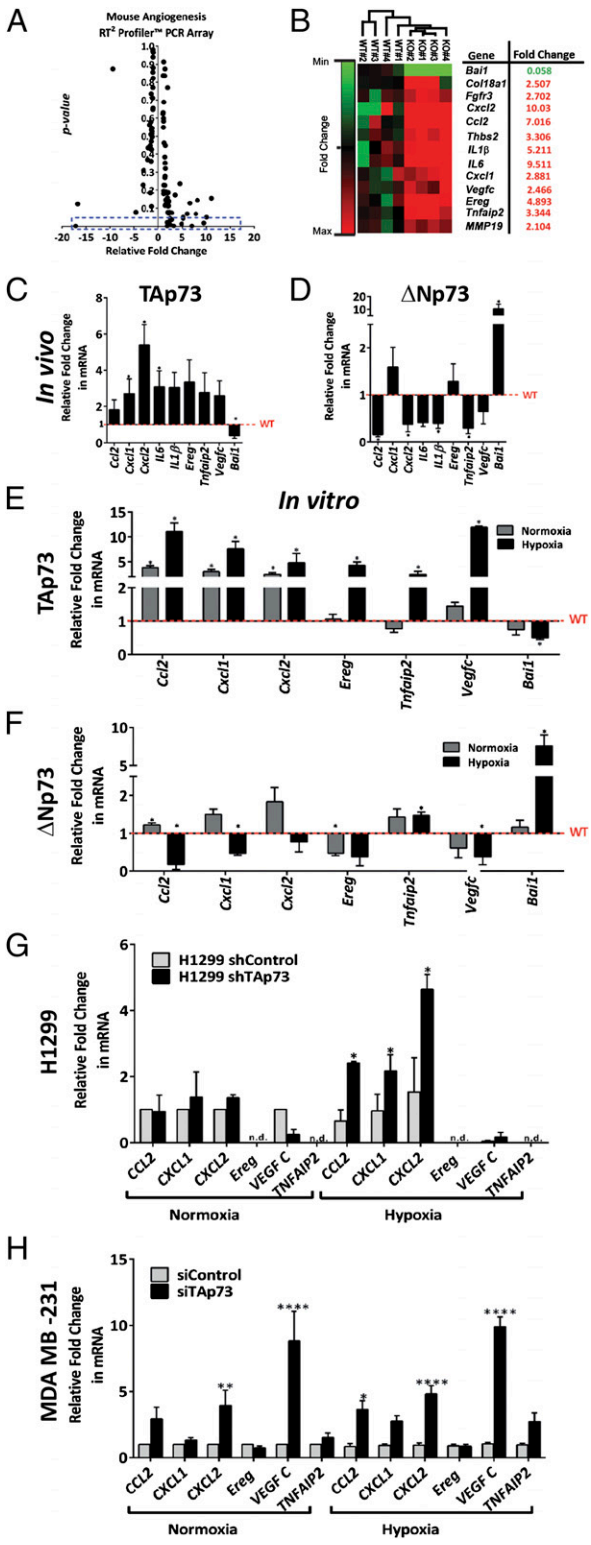

Fig. 3. Expression of angiogenic factors is controlled by p73 isoforms. (*A*) Volcano plot presenting angiogenic RT^2 profile PCR array data as relative fold-change of all 84 genes plotted against the *P* value (Student's *t test*). Vertical threshold reflects relative statistical significance ($P \leq 0{,}05$), and horizontal threshold reflects relative fold-change in gene expression ≥twofold difference between TAp73 WT and KO tumors (n = 4 tumors/group). (*B*) Heatmap showing fold change for genes that passed the threshold (red, high; green, low). (*C–F*) Validation of potential target genes using quantitative RT-PCR; results shown are the mean fold change ± SD relative to WT (red dotted line). (*C*) Genes confirmed to be deregulated in TAp73-deficient tumors compared with WT (n = 3 tumors/group). (*D*) Expression analysis of tumors derived from ΔNp73$^{-/-}$ or WT MEFs$^{E1A/Ras}$. Results shown are the mean fold change ± SD relative to WT (n = 3/group). Expression analysis of TAp73$^{-/-}$ MEFs$^{E1A/Ras}$ (*E*), ΔNp73$^{-/-}$MEFs$^{E1A/Ras}$ (*F*), H1299 cells with shRNA targeting TAp73 (*G*), and MDA MB-231 treated with siRNA against TAp73 (*H*), grown in vitro in normoxia (gray bars) or hypoxia for 24 h (black bars), normalized to 18S or 28S RNA and compared with WT cells. n.d., not detected.

(*Bai1*) (Fig. 3 *C–F*). The *Bai1* gene encodes a large transmembrane protein that contains several thrombospondin type 1 repeats, and its extracellular part can be cleaved into antiangiogenic peptides called vasculostatins (27). Reintroduction of TAp73α or TAp73β into TAp73$^{-/-}$ cells up-regulates *Bai1*, whereas ΔNp73α and ΔNp73β expression suppress Bai1 expression (Fig. S4 *A* and *B*). Furthermore, using H1299 cells with stable shRNA KD of TAp73 results in *BAI1* down-regulation (Fig. S4 *C* and *D*). In contrast, ectopic overexpression of TAp73 isoforms, and TAp73β in particular, increases *BAI1* expression in H1299 (Fig. S4*E*), suggesting it is a direct transcriptional target of TAp73. The *BAI1* gene has been reported to contain a putative p53-response element (p53RE) (28). Analysis of publically available p53 chromatin immunoprecipitation (ChIP)-sequencing data confirmed the presence of a p53RE in intron 10 of *BAI1*, and we also observed a putative p53RE in intron 10 of the mouse *Bai1* gene (Fig. S4*F*). Using ChIP, we could detect direct binding of endogenous TAp73 to intron 10 in *Bai1* (Fig. S4*G*). Furthermore, to determine whether TAp73 is directly activating Bai1 expression, *BAI1* intron 10 was cloned into a luciferase reporter and coexpressed with different p73 isoforms, as well as with p53. Ectopic expression of either TAp73β or p53 activated the Bai1 luciferase reporter. In contrast, ΔNp73 isoforms suppressed reporter activity (Fig. S4 *H* and *I*), indicating that *BAI1* is a direct target of TAp73β and p53 and that high levels of ΔNp73 inhibit its expression.

Shifting the Balance Between p73 Isoforms Correlates with Angiogenesis in Patients with Breast Cancer and Affects Accumulation of Hif-1α During Hypoxia. Next, we investigated whether the enhanced angiogenic phenotype we observed could be found in human cancer. TAp73 is rarely mutated or lost in human solid tumors; instead, ΔNp73 is often up-regulated, thus shifting the balance between the isoforms (1). Up-regulation of ΔNp73 has been associated with poor prognosis in breast cancer (18), and we therefore analyzed mRNA expression in 1,048 breast cancers from The Cancer Genome Atlas (TCGA) (29). Patient samples were separated by high or low ΔNp73 expression (99 vs. 449 patients), and through gene set enrichment analysis (GSEA), both angiogenesis and hypoxia signatures were associated with high ΔNp73 levels (Fig. 4*A* and Datasets S1 and S2), suggesting that shifting the balance between p73 isoforms toward ΔNp73 increases angiogenesis in human tumors.

The correlation between up-regulation of hypoxia-induced genes and high ΔNp73 levels was of particular interest, considering our findings that expression of proangiogenic target genes was further enhanced in TAp73$^{-/-}$ and repressed in ΔNp73$^{-/-}$ MEFs on hypoxia (Fig. 3 *E* and *F*). Transcriptional response to hypoxia occurs mainly through activation of the hypoxia-inducible factor (HIF) family of transcription factors. HIF-1α is normally rapidly degraded during normoxic conditions but is stabilized on hypoxia, dimerizes with HIF-1β, and translocates to the nucleus, where it binds to hypoxia-response elements (HRE) in target promoters (30). We thus analyzed the promoter region of the proangiogenic genes up-regulated in TAp73$^{-/-}$ cells and found that all of them contained HRE, and that this regulation was conserved between mouse and human (Fig. S5), suggesting that expression of HIF-target genes is enhanced on TAp73 loss. To confirm that they indeed are direct Hif-1α target genes, we performed ChIP, using anti-Hif-1α and normal IgG on chromatin

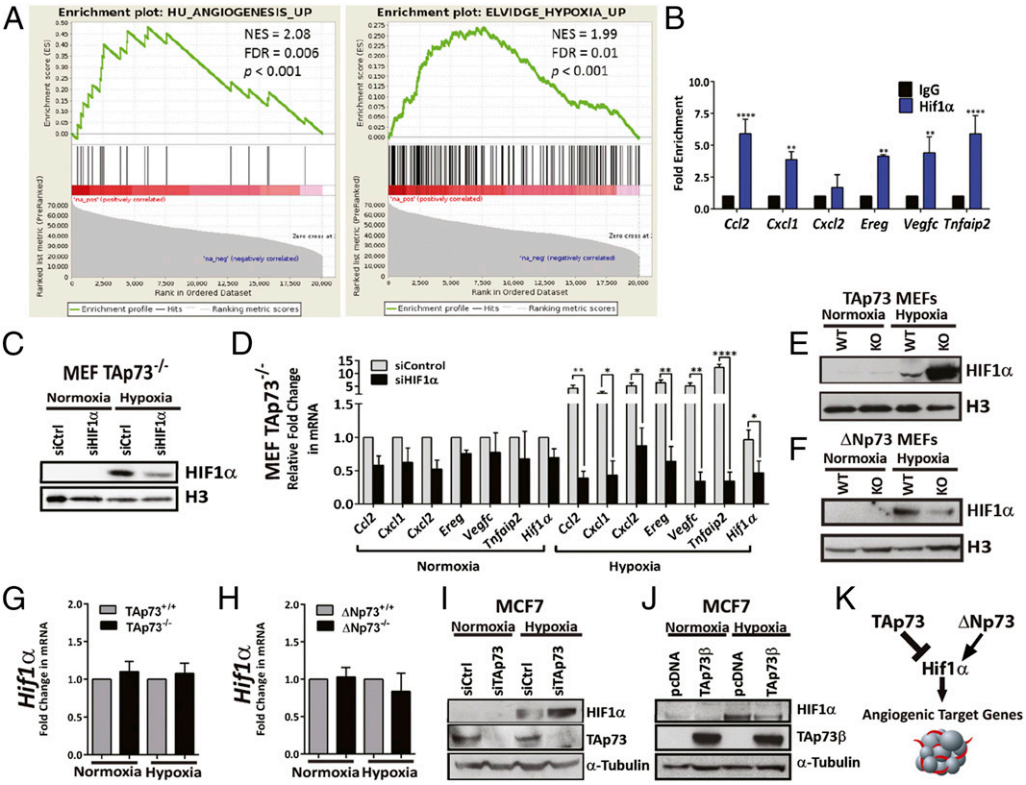

Fig. 4. Shifting the balance between p73 isoforms correlates with angiogenesis in patients with breast cancer and affects accumulation of Hif-1α during hypoxia. (*A*) GSEA was performed with two different gene sets: angiogenesis gene set ($n = 21$) (31) and hypoxia gene set ($n = 171$) (32). "Signal-to-Noise" ratio statistic was used to rank genes according to their correlation with high levels of ΔNp73 (red); genes on the left correlate most with ΔNp73. The vertical black lines indicate the positions of genes in the studied gene set in an ordered, nonredundant data set. The green curve represents the enrichment score curve obtained by the GSEA software. Breast cancer samples expressing high levels of ΔNp73 show increased expression of angiogenesis genes and genes up-regulated by hypoxia (GSEA $P < 0.001$) (*B*) ChIP-qPCR, enrichment fold increase in TAp73$^{-/-}$ MEFs$^{E1A/Ras}$ for Hif-1α predicted targets. Five independent experiments are combined. $P \leq 0.05$; $^{**}P \leq 0.01$; $^{***}P \leq 0.001$; $^{****}P \leq 0.0001$. (*C*) Western blot analysis of nuclear extracts isolated from TAp73$^{-/-}$ MEFs$^{E1A/Ras}$ treated with siHIF1α and grown in hypoxia and normoxia for 12 h. (*D*) Expression analysis of genes in TAp73$^{-/-}$ MEFs$^{E1A/Ras}$ siControl (gray bars) and in TAp73$^{-/-}$ MEFs$^{E1A/Ras}$ siHIF1α (black bars) grown in normoxia and hypoxia for 12 h; samples are normalized to 18S RNA and compared with siControl normoxia cells. Western blot showing Hif-1α accumulation after 12 h hypoxia in (*E*) TAp73$^{-/-}$ MEFs$^{E1A/Ras}$ and (*F*) ΔNp73$^{-/-}$ MEFs$^{E1A/Ras}$. (*G* and *H*) Hif-1α mRNA in hypoxic and normoxic TAp73$^{-/-}$ and ΔNp73$^{-/-}$ MEF$^{E1A/Ras}$ cells relative to WT cells. Western blot showing Hif-1α protein in MCF7 cells treated with (*I*) siTAp73 or (*J*) TAp73 overexpression. (*K*) Schematic model of p73 isoforms opposing effect on Hif-1α, and thus deregulating angiogenic target genes.

derived from TAp73$^{-/-}$ cells grown in hypoxic conditions. As expected, endogenous Hif-1α was found bound to all target gene promoters, with the exception of Cxcl2 (Fig. 4*B*), demonstrating that they are Hif-1α target genes. To further validate the dependence on Hif-1α, we used siRNA to KD Hif-1α in TAp73$^{-/-}$ cells (Fig. 4*C*) and assessed the expression of target genes in both normoxia and hypoxia. Importantly, all target genes were severely down-regulated in hypoxia on Hif-1α KD, showing they are regulated by Hif-1α (Fig. 4*D*).

Next, we investigated whether TAp73 and ΔNp73 had a direct effect on Hif-1α levels. Considering the tight regulation of HIF-1α protein, we analyzed its accumulation in response to hypoxia and found a significant increase in TAp73$^{-/-}$ cells compared with WT (Fig. 4*E*), whereas HIF-1α protein levels decreased in ΔNp73$^{-/-}$ cells compared with WT (Fig. 4*F*). We did not observe any differences in *Hif-1α* mRNA levels on deletion of either TAp73 or ΔNp73 (Fig. 4 *G* and *H*), suggesting p73 isoforms regulate Hif-1α protein stability, rather than its expression in response to hypoxia. HIF-1α protein accumulation on TAp73 loss was also confirmed in MCF7 cells treated with siRNA against TAp73 (Fig. 4*I*). In contrast, overexpression of TAp73 down-regulates HIF-1α levels (Fig. 4*J*), suggesting TAp73 normally inhibits HIF-1α protein accumulation in response to hypoxia and that on TAp73 loss, HIF-1α protein levels increases, resulting in enhanced activation of proangiogenic HIF-1α target genes (Fig. 4*K*).

Discussion

Angiogenesis is essential for the growing tumor, supplying it with oxygen, nutrients, and factors that contribute to the propagation and metastatic spread. The role of p73 isoforms during tumor development has been extensively studied. TAp73 has been shown to induce cell cycle arrest, differentiation, and apoptosis, as well as to suppress aneuploidy (reviewed in ref. 1), thus acting as a tumor suppressor. In contrast, ΔNp73 is found to have oncogenic properties and promotes cell transformation and metastasis (10, 12). However, their function in tumor angiogenesis is still poorly understood. Here we report that TAp73 and ΔNp73 have opposing roles during tumor angiogenesis. Loss of TAp73 isoforms results in highly vascularized tumors, a phenotype that is reversed in ΔNp73$^{-/-}$ tumors. This is further supported by transcriptome analysis of human breast cancer samples that shows correlation between up-regulated levels of ΔNp73 and an angiogenic signature.

In addition, we show that the angiogenic effect is not dependent on tumor size but, rather, is the result of a direct effect on endothelial cell sprouting and vascular permeability, indicating that TAp73 and ΔNp73 are regulating angiogenic factors produced by the tumors cells in an opposing manner. The transition of a tumor from an avascular to a vascular state is characterized by the up-regulation of proangiogenic factors. In

TAp73$^{-/-}$ cells, as well as in human cancer cells with TAp73 KD, we observed up-regulation of Ccl2, Cxcl1, Cxcl2, and VEGF-C, all of which are known to promote tumor angiogenesis. Moreover, we found the angiogenesis inhibitor Bai1 to be a direct transcriptional target of TAp73β and p53 and to be inhibited by ΔNp73.

Classically considered a lymphangiogenic factor, VEGF-C has also been reported to induce angiogenesis through the activation of the VEGF-R2 receptor on endothelial cells (24). The VEGF-C/VEGF-R2 axis also enhances vascular permeability by increasing VE-cadherin internalization, thus destabilizing adherence junctions between ECs (26). Here we show that the VE-cadherin signal is severely reduced in ECs treated with conditioned medium from TAp73$^{-/-}$ cells. In addition to finding increased *Vegfc* mRNA levels in TAp73$^{-/-}$ cells, we also observed enhanced secretion of VEGF-C from TAp73$^{-/-}$ cells (Fig. S6). Taken together, the elevated expression of VEGF-C in TAp73-deficient tumors and cells may explain the increase in vascular permeability observed both in vitro and in vivo.

Interestingly, all proangiogenic genes found up-regulated in TAp73-deficient cells have HRE in their promoter regions. In addition, gene set enrichment analysis of human breast cancer samples correlated hypoxia-up-regulated genes with up-regulation of ΔNp73, suggesting p73 isoforms control HIF-1α activity. HIF-1α normally increases in human tumors, and its expression has been correlated with poor patient outcome in a wide variety of tumors, showing that HIF-1α up-regulation is a frequent event during tumorigenesis and that it drives tumor progression (30). HIF-1α levels are normally kept low through oxygen-dependent ubiquitin-mediated protesomal degradation. When oxygen levels drop, HIF-1α gets stabilized and translocates into the nucleus, where it binds to HRE and induces expression of genes involved in angiogenesis, proliferation, metastasis, and metabolism (30). We observed that TAp73 overexpression or ΔNp73 loss reduced the accumulation of HIF-1α protein during hypoxia, a finding that was reversed on TAp73 loss, thus showing that p73 isoforms directly control HIF-1α activity. Furthermore, using ChIP assay and siRNA targeting HIF-1α, we show that the expression of the proangiogenic cytokines found up-regulated in TAp73$^{-/-}$ cells is dependent on HIF-1α and that they are direct HIF-1α target genes.

In conclusion, we have found that p73 isoforms have an important role in controlling tumor angiogenesis through regulating the paracrine signaling between tumor cells and the surrounding tumor microenvironment. Our data demonstrate that TAp73 loss or ΔNp73 up-regulation enhance HIF-1α activity and secretion of cytokines from tumor cells that induce endothelial sprouting toward the tumor cells, increase vascular permeability, and support tumor progression.

Materials and Methods

Tumor growth and angiogenesis were studied using s.c. injections of transformed cells in athymic nude mice and in the EμMyc B-cell lymphoma mouse model crossed with TAp73$^{-/-}$, ΔNp73$^{-/-}$, or p73$^{+/+}$ mice. Endothelial cell sprouting was studied in vivo, using tumor cells grafted into transgenic zebrafish. Gene expression was analyzed by quantitative RT-PCR, and HIF-1α accumulation was analyzed by Western blot. Binding of Hif1α and TAp73 to HRE or p53RE was analyzed by ChIP. Correlations between p73 isoform expression and angiogenesis in clinical breast cancer samples were analyzed, using publically available RNA sequencing data from the TCGA repository. Detailed material and methods are provided in *SI Materials and Methods*.

ACKNOWLEDGMENTS. We thank Prof. Galina Selivanova, Prof. Lorenz Poellinger, Dr. Ulrica Westermark, Prof. Yihai Cao, Dr. Pegah Rouhi, Dr. Kayoko Hosaka, Prof. Kristian Pietras, Dr. Katarina Gradin, Dr. Anita Göndör, Dr. Franziska Boettger, and Patrik Andersson for helpful discussions, technical advice, and reagents. We thank Martina Czapko, Elin Edsbäcker, Rafael Galupa, and Anja Waldmann for technical support. We are also grateful for the excellent help from Kjell Hultenby and the electron microscopy facility at Karolinska Institutet. This work was supported by grants from the Swedish Research Council, the Swedish Cancer Society, the Swedish Childhood Cancer Foundation, and the Åke Wiberg, O. E. and Edla Johansson, and Magn. Bergwall foundations. H.A.M.S., H.Z., and A.M. are funded by Karolinska Institutet doctoral grants. A.F.-W. is supported by the Knut and Alice Wallenberg Foundation. M.T.W. is supported by an assistant professorship from the Swedish Research Council and a Young Investigator Award from the Swedish Cancer Society.

1. Rufini A, et al. (2011) p73 in Cancer. *Genes Cancer* 2(4):491–502.
2. Grob TJ, et al. (2001) Human delta Np73 regulates a dominant negative feedback loop for TAp73 and p53. *Cell Death Differ* 8(12):1213–1223.
3. Tomasini R, et al. (2008) TAp73 knockout shows genomic instability with infertility and tumor suppressor functions. *Genes Dev* 22(19):2677–2691.
4. Tomasini R, et al. (2009) TAp73 regulates the spindle assembly checkpoint by modulating BubR1 activity. *Proc Natl Acad Sci USA* 106(3):797–802.
5. Rodhe J, Kavanagh E, Joseph B (2013) TAp73β-mediated suppression of cell migration requires p57Kip2 control of actin cytoskeleton dynamics. *Oncotarget* 4(2):289–297.
6. Tamura M, et al. (2014) Forkhead transcription factor FOXF1 is a novel target gene of the p53 family and regulates cancer cell migration and invasiveness. *Oncogene* 33(40):4837–4846.
7. Chen X, et al. (2013) Gene expression of WWOX, FHIT and p73 in acute lymphoblastic leukemia. *Oncol Lett* 6(4):963–969.
8. Nemajerova A, Petrenko O, Trümper L, Palacios G, Moll UM (2010) Loss of p73 promotes dissemination of Myc-induced B cell lymphomas in mice. *J Clin Invest* 120(6):2070–2080.
9. Siu LL, Chan JK, Wong KF, Kwong YL (2002) Specific patterns of gene methylation in natural killer cell lymphomas: P73 is consistently involved. *Am J Pathol* 160(1):59–66.
10. Petrenko O, Zaika A, Moll UM (2003) deltaNp73 facilitates cell immortalization and cooperates with oncogenic Ras in cellular transformation in vivo. *Mol Cell Biol* 23(16):5540–5555.
11. Wilhelm MT, et al. (2010) Isoform-specific p73 knockout mice reveal a novel role for delta Np73 in the DNA damage response pathway. *Genes Dev* 24(6):549–560.
12. Steder M, et al. (2013) DNp73 exerts function in metastasis initiation by disconnecting the inhibitory role of EPLIN on IGF1R-AKT/STAT3 signaling. *Cancer Cell* 24(4):512–527.
13. Uramoto H, et al. (2004) Expression of deltaNp73 predicts poor prognosis in lung cancer. *Clin Cancer Res* 10(20):6905–6911.
14. Zitterbart K, et al. (2007) p73 expression in medulloblastoma: TAp73/DeltaNp73 transcript detection and possible association of p73alpha/DeltaNp73 immunoreactivity with survival. *Acta Neuropathol* 114(6):641–650.
15. Soldevilla B, et al. (2014) Tumor-derived exosomes are enriched in ΔNp73, which promotes oncogenic potential in acceptor cells and correlates with patient survival. *Hum Mol Genet* 23(2):467–478.
16. Leung TH, et al. (2013) The interaction between C35 and ΔNp73 promotes chemoresistance in ovarian cancer cells. *Br J Cancer* 109(4):965–975.
17. Guan M, Peng HX, Yu B, Lu Y (2003) p73 Overexpression and angiogenesis in human colorectal carcinoma. *Jpn J Clin Oncol* 33(5):215–220.
18. Domínguez G, et al. (2006) DeltaTAp73 upregulation correlates with poor prognosis in human tumors: Putative in vivo network involving p73 isoforms, p53, and E2F-1. *J Clin Oncol* 24(5):805–815.
19. Beitzinger M, et al. (2008) p73 poses a barrier to malignant transformation by limiting anchorage-independent growth. *EMBO J* 27(5):792–803.
20. Adams JM, et al. (1985) The c-myc oncogene driven by immunoglobulin enhancers induces lymphoid malignancy in transgenic mice. *Nature* 318(6046):533–538.
21. Nicoli S, Ribatti D, Cotelli F, Presta M (2007) Mammalian tumor xenografts induce neovascularization in zebrafish embryos. *Cancer Res* 67(7):2927–2931.
22. Le Guelte A, Gavard J (2011) Role of endothelial cell-cell junctions in endothelial permeability. *Methods Mol Biol* 763:265–279.
23. Millán J, et al. (2010) Adherens junctions connect stress fibres between adjacent endothelial cells. *BMC Biol* 8:11.
24. Cao Y, et al. (1998) Vascular endothelial growth factor C induces angiogenesis in vivo. *Proc Natl Acad Sci USA* 95(24):14389–14394.
25. Amin DN, Hida K, Bielenberg DR, Klagsbrun M (2006) Tumor endothelial cells express epidermal growth factor receptor (EGFR) but not ErbB3 and are responsive to EGF and to EGFR kinase inhibitors. *Cancer Res* 66(4):2173–2180.
26. Azzi S, Hebda JK, Gavard J (2013) Vascular permeability and drug delivery in cancers. *Front Oncol* 3:211.
27. Kaur B, Brat DJ, Devi NS, Van Meir EG (2005) Vasculostatin, a proteolytic fragment of brain angiogenesis inhibitor 1, is an antiangiogenic and antitumorigenic factor. *Oncogene* 24(22):3632–3642.
28. Nishimori H, et al. (1997) A novel brain-specific p53-target gene, BAI1, containing thrombospondin type 1 repeats inhibits experimental angiogenesis. *Oncogene* 15(18):2145–2150.
29. Cancer Genome Atlas Network (2012) Comprehensive molecular portraits of human breast tumours. *Nature* 490(7418):61–70.
30. Rankin EB, Giaccia AJ (2008) The role of hypoxia-inducible factors in tumorigenesis. *Cell Death Differ* 15(4):678–685.
31. Hu J, et al. (2005) Gene expression signature for angiogenic and nonangiogenic non-small-cell lung cancer. *Oncogene* 24(7):1212–1219.
32. Elvidge GP, et al. (2006) Concordant regulation of gene expression by hypoxia and 2-oxoglutarate-dependent dioxygenase inhibition: The role of HIF-1alpha, HIF-2alpha, and other pathways. *J Biol Chem* 281(22):15215–15226.